cigre Turkey

TEPES
TURKISH JOURNAL OF ELECTRICAL POWER AND ENERGY SYSTEMS

TEPES, Vol. 3, Issue. 1, 47-60, 2023 **DOI:** 10.5152/tepes.2023.23001

RESEARCH ARTICLE

Sensitivity and Cost Analysis of a Microgrid With a Day-Ahead Energy Management System

Sezai Polat[1], Emrah Bıyık[2], Hacer Şekerci Öztura[3]

[1]Department of Electrical and Electronics Engineering, Graduate School, Yaşar University, İzmir, Turkey
[2]Department of Energy Systems Engineering, Yaşar University, İzmir, Turkey
[3]Department of Electrical and Electronics Engineering, Yaşar University, İzmir, Turkey

Cite this article as: S. Polat, E. Bıyık and H. Şekerci Öztura, Sensitivity and cost analysis of a microgrid with a day-ahead energy management system, *Turk J Electr Power Energy Syst.,* 2023; 3(1), 47-60.

ABSTRACT

The use of renewable energy sources (RESs) can ensure both lower cost of energy and improvement in voltage levels in the grid. Likewise, batteries can help achieve technical improvement and cost reduction. However, the full benefits of integrating RESs and batteries into the grid can only be realized by a suitable energy management system (EMS). In this work, a predictive EMS is developed to optimally operate a microgrid (MG) with photovoltaics and batteries while satisfying voltage constraints in the distribution grid. First, mathematical models of the MG components are obtained. Then, proper load flow method is selected for the network structure. Using component models and the load flow method, a day-ahead EMS is posed as an optimization problem. Since the power flow calculations are nonlinear, the optimization problem is constructed as a nonlinear program. Simulation studies are performed to analyze the sensitivity of the cost of operation and power loss in the grid, with respect to different system parameters. It is confirmed that the purchase price of electricity and the amount of photovoltaic panels were the most effective factors on the daily energy cost.

Index Terms— Battery, day-ahead, microgrid

I. INTRODUCTION

The share of renewable energy sources (RESs) which represents the sum of solar and wind energies in the world increased from 2% in 2011 to 10% in 2021 [1]. Increasing use of renewable energy can help to reduce the energy costs as well as energy loss. Besides these benefits, some technical issues arise with the integration of distributed generation (DG) [2]. The increase in the number of equipment used, such as photovoltaic (PV) panel, wind turbine, and battery, complicates power dispatch problem [3]. The power dispatch problem can be solved by day-ahead scheduling [4]. There are some technical limits and constraints that should be taken into account while tackling this problem. In order to offer cost-effective and technical options to power systems, day-ahead energy management systems (EMSs) are frequently used. Since the effect of energy sources and loads on system security should be estimated, power flow calculations (PFCs) are important for power dispatch scheduling in EMS. Power flow calculation needs to be considered when operating within technical limits and achieving low energy cost in grid.

There are different methods developed in the literature for PFCs [5]. In [6], the authors analyzed the reduction of energy cost in a radial distribution system (RDS) by using the DistFlow PFC method. In [7], the authors carried out a study aiming to reduce energy costs in an RDS with different DG sources by using direct current PFC. In [8], instead of cost minimization, line loss and voltage fluctuations were aimed to be minimized by using the Newton–Raphson PFC method. In [9], the authors carried out a study aimed at minimizing the total voltage regulation cost for RDS, including mobile battery system and on-load tap changer, by using the DistFlow method. Another PFC method is a direct approach-based load flow solution. [10]. In addition to energy cost reduction, PFC is also used for the placement problem of the DG [11], for the optimum operation of the battery [12], for the improvement of voltage profile [13], for optimal network reconfiguration in [14], and for optimal placement of battery storage systems and capacitor banks in grid [15].

Forecast of energy cost is as important as estimation for staying within electrical specifications. Therefore, EMS optimization is a

Corresponding author: Sezai Polat, **E-mail:** sezaipolat@gmail.com

Received: January 2, 2023
Accepted: January 18, 2023

very important issue. Day-ahead EMS performs economic dispatch for each hour of the following day. A robust and efficient PFC method is required when considering the number and size of the system equipment. Direct approach-based load flow solution is a rapid and enough precision method for RDS [16, 17].

To this direction, integration of PV and battery energy storage systems (BESSs) into the grid can help to decrease energy cost and energy losses and improve voltage profiles [18, 19].

This study aims to decrease the energy cost by integrating PVs and BESSs into the IEEE 33 bus test system. The decrease in the daily operating cost includes minimizing the line losses, the cost of energy bought from the grid, and the BESS operating cost and maximizing the revenue of sales to the grid. In this paper, various simulation studies are carried out by creating an optimization model that purposes at the lowest energy cost and losses without exceeding the voltage limits of buses for 24 h, according to the load and RESs obtained by day-ahead EMS.

This paper expands the work reported in [20] in three directions: 1) comparison of the power flow algorithm with the literature, 2) minimization of power loss and daily energy cost, and 3) sensitivity analysis of the cost and power loss characteristics of the EMS.

The major contributions of this study, as compared to similar studies, are:

1) Tackling operational cost optimization and power quality (voltage regulation) concurrently in the EMS by using the distribution load flow (DLF) technique for a multi-period power flow in a microgrid (MG).
2) Analyzing the effects of system parameters (electricity prices, PV parameters, and BESS cost and capacities) for sensitivity analysis for daily energy cost and power loss.

The rest of this paper is organized as follows. The MG structure is presented in Section II. Power flow analysis is stated in Section III. Section IV presents the day-ahead optimization model of a MG. The case studies, analysis of the results, and sensitivity analysis are given in Section V. Lastly, conclusions are given in Section VI.

Main Points

- A predictive energy management system (EMS) is developed to optimally operate a microgrid with photovoltaics (PVs) and battery energy storage systems (BESSs), while voltage constraints are satisfied in the distribution grid.
- The operational cost optimization and power quality (voltage regulation) are tackled concurrently in the EMS by using the distribution load flow technique for a multi-period power flow.
- The effects of the system parameters (e.g., electricity prices, PV parameters, and BESS cost and capacities) are analyzed for sensitivity analysis, daily energy cost, and power loss.

II. MICROGRID

The MG is defined Distributed Energy Resources (DER) and interconnected loads, whose electrical properties are defined within certain limits, which can be controlled and acted as a single controllable network equipment [21]. A simple structure of an MG is shown in Fig. 1.

Microgrids may include RESs such as PV and wind energy when geographic location is considered. In addition, it may also include a battery and/or generator to supply the energy requirement of the load uninterruptedly at a lower cost.

An EMS fulfills the role to supply the loads within electrical technical limits in the MG. In addition, EMS objectives include reducing the cost of energy and even making a profit. In other words, the MG needs a control system which is responsible for operating the equipment optimally while fulfilling the required quality parameters of electricity.

The day-ahead planning allows power dispatch in the MG for the following day by using RES forecast and load forecast data. This planning should calculate the power generations, loads, and energy loss in the MG.

Because of the reasons explained above, a precise and simple modeling is the most important issue for EMS. In this study, mathematical models are formulated for objective function, including constraints, PV model, BESS model, and PFC for MG and also for constraints.

A. Photovoltaic System

Different calculation methods for PV power output estimation were investigated in [22, 23]. However, (1) can be used for PV power calculation at time t for its simplicity, low computational burden, and faster computation [24]. Photovoltaics generate electricity in a direct proportion to the global solar radiation and surface area by means of (1).

$$P_t^{PV} = \eta_{pv}.A_{pv}.G_t^{PV} \qquad \forall t \tag{1}$$

where P_t^{PV} is the generated power by PV panel, η_{Pv} and A_{Pv} are the efficiency and area of PV panel, respectively, and G_t^{PV} is the solar irradiance.

B. Battery Energy Storage System

Renewable energy source power outputs may be intermittent because of the uncertain nature of renewable energy. Battery energy store system can be used for energy supply when energy generation is intermittent and fluctuating. Additionally, BESS can provide economic benefits because it can reduce the cost of the energy purchased from the grid and increase the sales revenue to the grid. The energy balance in the BESS is given in (2) [25].

$$SoC_{t+1}^{BESS} = SoC_t^{BESS} + \eta_{BC}.P_t^{BC}.\Delta t - \frac{P_t^{BD}}{\eta_{BD}}.\Delta t \qquad \forall t \tag{2}$$

where SoC_t^{BESS} means the battery state of charge. η_{BC} and η_{BD} are the charge/discharge efficiency of the BESS. P_t^{BC} and P_t^{BD} are charge/discharge power of the BESS, and Δt is the time interval.

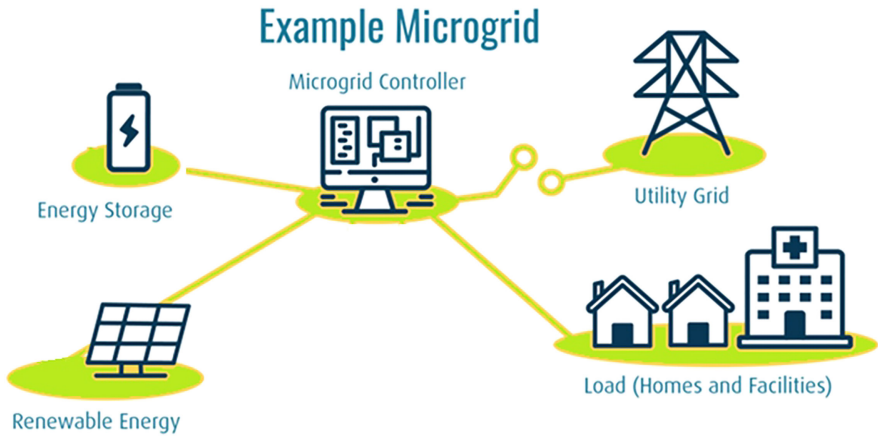

Fig. 1. Structure of studied MG in this paper (modified from [22]).

BESS charge and discharge powers must be within a certain range in (3) and (4).

$$0 \le P_t^{BC} \le P^{BC,max} \qquad \forall t \tag{3}$$

$$0 \le P_t^{BD} \le P^{BD,max} \qquad \forall t \tag{4}$$

where $P^{BC,\max}$ and $P^{BD,\max}$ are the maximum power of the BESS in charging/discharging mode, respectively.

III. POWER FLOW ANALYSIS

The Newton–Raphson, Gauss–Seidel, and fast-decoupled methods, which are known power flow models, cannot be applied because of the high R/X ratio of distribution systems [26]. These techniques do not give high precision results, and it takes a long time [27]. For this reason, other PFC methods are used for RDS in the literature. Distribution load flow is one of the mostly used methods for RDS [10].

A. Distribution Load Flow Method

The DLF method is recommended for RDS. In this method, calculations are carried out by creating the bus injection to branch current (BIBC) and the branch current to bus voltage (BCBV) matrices.

The apparent power is calculated at bus i at t time in a distribution network by (5).

$$S_{i,t} = P_{i,t} + jQ_{i,t} \qquad \forall t,i \tag{5}$$

where $P_{i,t}$ and $Q_{i,t}$ mean the active and reactive power at bus i, at time t, respectively.

Since the apparent power S_i and V_i voltage of bus i are known, the load currents I_i can be calculated by (6).

$$I_{i,t} = \left(\frac{S_{i,t}}{V_{i,t}}\right)^* \qquad \forall t,i \tag{6}$$

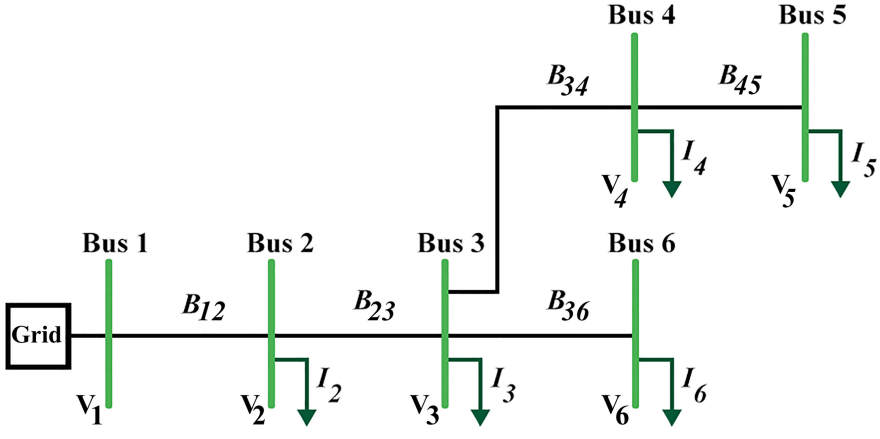

Fig. 2. Example of an RDS with six buses.

Fig. 2 represents a six-bus radial system. If the recommended DLF technique is applied, the calculation is performed in the following steps.

The line currents B_{ij} are calculated using the bus currents I_i, by applying Kirchhoff's law of currents. Line currents are obtained from (7);

$$\begin{aligned} B_{12} &= I_2 + I_3 + I_4 + I_5 + I_6 \\ B_{23} &= I_3 + I_4 + I_5 + I_6 \\ B_{34} &= I_4 + I_5 \\ B_{45} &= I_5 \\ B_{36} &= I_6 \end{aligned} \tag{7}$$

Equation (8) given above can be written in a matrix form as follows:

$$\begin{bmatrix} B_{12} \\ B_{23} \\ B_{34} \\ B_{45} \\ B_{36} \end{bmatrix} = \begin{bmatrix} 1 & 1 & 1 & 1 & 1 \\ 0 & 1 & 1 & 1 & 1 \\ 0 & 0 & 1 & 1 & 0 \\ 0 & 0 & 0 & 1 & 0 \\ 0 & 0 & 0 & 0 & 1 \end{bmatrix} . \begin{bmatrix} I_2 \\ I_3 \\ I_4 \\ I_5 \\ I_6 \end{bmatrix} \tag{8}$$

$$[B] = [BIBC].[I] \tag{9}$$

Equation (10) using line currents to calculate bus voltages is given below.

$$\begin{aligned} V_2 &= V_1 - B_{12}.Z_{12} \\ V_3 &= V_2 - B_{23}.Z_{23} \\ V_4 &= V_3 - B_{34}.Z_{34} \\ V_4 &= V_1 - B_{12}.Z_{12} - B_{23}.Z_{23} - B_{34}.Z_{34} \end{aligned} \tag{10}$$

where V_i is voltage magnitude at bus i and Z_{ij} is the line impedance between bus i and j. Similarly, the voltage difference in terms of line currents can be obtained from (11).

$$\begin{bmatrix} V_1 \\ V_1 \\ V_1 \\ V_1 \\ V_1 \end{bmatrix} - \begin{bmatrix} V_2 \\ V_3 \\ V_4 \\ V_5 \\ V_6 \end{bmatrix} = \begin{bmatrix} Z_{12} & 0 & 0 & 0 & 0 \\ Z_{12} & Z_{23} & 0 & 0 & 0 \\ Z_{12} & Z_{23} & Z_{34} & 0 & 0 \\ Z_{12} & Z_{23} & Z_{34} & Z_{45} & 0 \\ Z_{12} & Z_{23} & 0 & 0 & Z_{36} \end{bmatrix} . \begin{bmatrix} B_{12} \\ B_{23} \\ B_{34} \\ B_{45} \\ B_{36} \end{bmatrix} \tag{11}$$

$$[\Delta V] = [BIBC].[B] \tag{12}$$

$$\left[\Delta V\right] = \left[BCBV\right].\left[BIBC\right].\left[I\right] \tag{13}$$

$$[\Delta V] = [DLF].[I] \tag{14}$$

The voltage differences between first bus and other buses can be obtained by the DLF matrix consisting of BIBC and BCBV matrices. The voltage differences and voltage magnitude at all buses are calculated iteratively as follows:

$$\left[\Delta V^{k+1}\right] = \left[DLF\right].\left[I^{k}\right] \tag{15}$$

$$\left[V^{k+1}\right] = V^{0} - \left[\Delta V^{k+1}\right] \tag{16}$$

Fig. 3 gives the flowchart of a PFC procedure.

The line current B_{ij} of each branch is calculated using PFC, and the losses in the lines can easily be calculated by using (17).

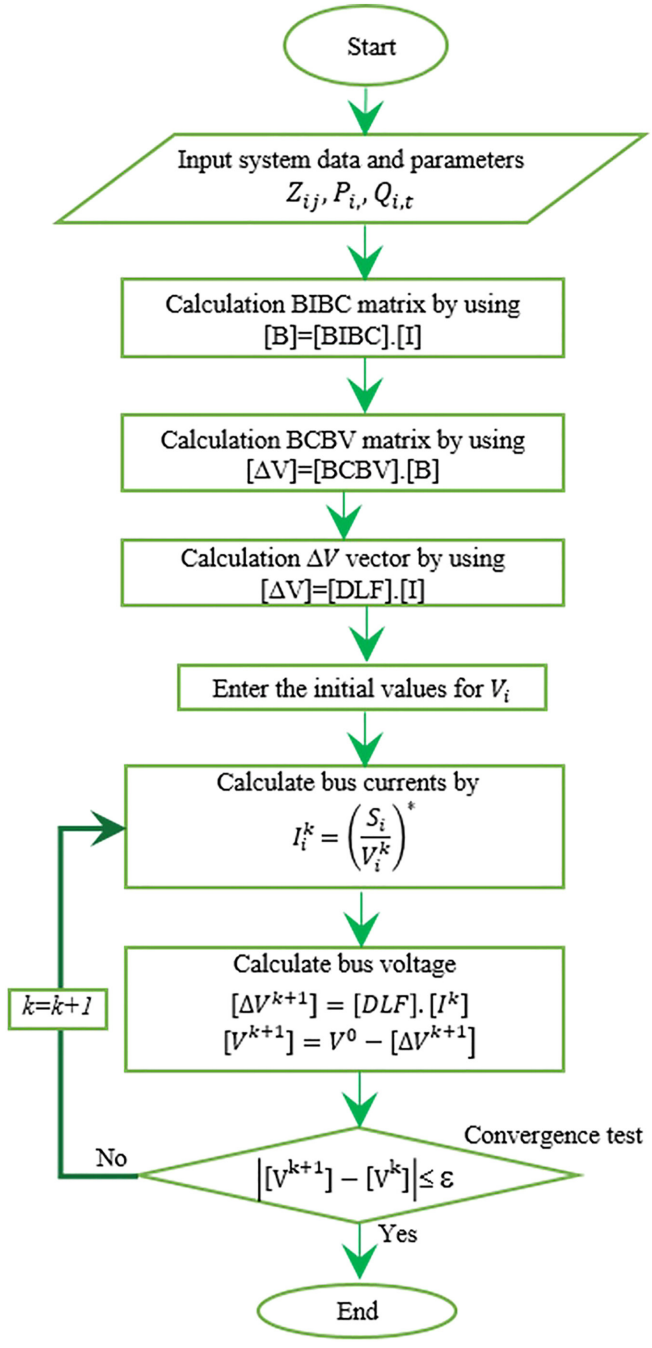

Fig. 3. Simplified flowchart of power flow.

$$P_{ij,t}^{loss} = r_{ij}.B_{ij,t}^{2} \qquad \forall i,j,t \tag{17}$$

where $P_{ij,t}^{loss}$, $B_{ij,t}$, and r_{ij} are line loss, line current at time t, and line resistance between bus i and j, respectively.

B. Demonstration of Distribution Load Flow Method

The recommended PFC is simulated on the IEEE 33 bus radial distribution test system in Fig. 4. The system has contains 32 lines and 33 buses, a voltage of 12.66 kV, 3.715 MW and 2.3 MVar load. The data of the test system can be seen in [11].

There are different power flow studies in the literature appropriate for the radial system. The new analytical formulations (analytical method) were developed for solving RDS in [14]. The backward and forward sweep method was presented in [28] for solving RDS. The dynamic data matrix method was proposed for calculating the voltages of buses by the authors in [29]. In [30], the authors proposed the direct backward/forward sweep solution technique to solve for PFC.

For the sake of recommended methodology (DLF technique) validation, the bus voltages and total power loss are tabulated in Table I and Table II, respectively. The comparison of voltages at each bus for different power flow methods is represented in Fig. 5.

It is seen that there is a negligible difference between the method applied in this study and the other methods. The used approach is validated with the results of the other methods in the test system.

This study is currently being expanded to include multi-period PFCs. In this paper, an optimization model to arrive at a day-ahead optimal plan for EMS is proposed and discussed. The model was simulated with historical weather data and forecasted load given in [31]. The forecasted load and power losses are depicted in Fig. 6. Total energy loss was calculated as 2733 kWh for 1 day.

IV. DAY-AHEAD OPTIMIZATION MODEL

A. The Objective Function

Fig. 7 illustrates the input–output scheme of a MG EMS system. It is aimed to minimize the operating costs by using the optimization problem in (18)–(20). The objective function includes minimizing expenses for power bought from grid, minimizing BESS operational cost, and maximizing revenue from selling to grid and also reducing line losses.

$$\min F = C_{GC} + C_{BC} \tag{18}$$

$$C_{GC} = \sum_{t=1}^{T} \left(\underbrace{P_t^{GB}.\lambda_t^{pp}}_{cost} - \underbrace{P_t^{GS}.\lambda_t^{SP}}_{revenue} \right).t \qquad \forall t \tag{19}$$

$$C_{BC} = \sum_{t=1}^{T} \sum_{n=1}^{N_{BESS}} \underbrace{\left(P_t^{BC}.\beta_{CC} + P_t^{BD}.\beta_{DC} \right)}_{cost}.t \qquad \forall t,n \tag{20}$$

where C_{GC} and C_{BC} are grid and BESS operational costs, respectively. P_t^{GB} and P_t^{GS} are power bought from grid and power sold to grid. λ_t^{pp} and λ_t^{SP} are the buying and selling price electricity. β_{CC} and β_{DC} are the charged and discharged degradation cost of BESS, respectively.

B. Constraints

1) Power Balance Constraint

The power balance equation is given in (21):

$$P_t^{GB} - P_t^{GS} - \sum_{n=1}^{N_{BESS}} P_t^{BC} + \sum_{n=1}^{N_{BESS}} P_t^{BD} + \sum_{n=1}^{N_{PV}} P_t^{PV} = \sum_{Load} P_{i,t}^{Load} + \sum_{Loss} P_{ij,t}^{loss} \qquad \forall t,i,j,n \tag{21}$$

where $\sum P_{i,t}^{Load}$ is equivalent to total active power at all buses at time t. Similarly, $\sum_{n=1}^{N_{BESS}} P_t^{BC}$ and $\sum_{n=1}^{N_{BESS}} P_t^{BD}$ mean sum of the charge and

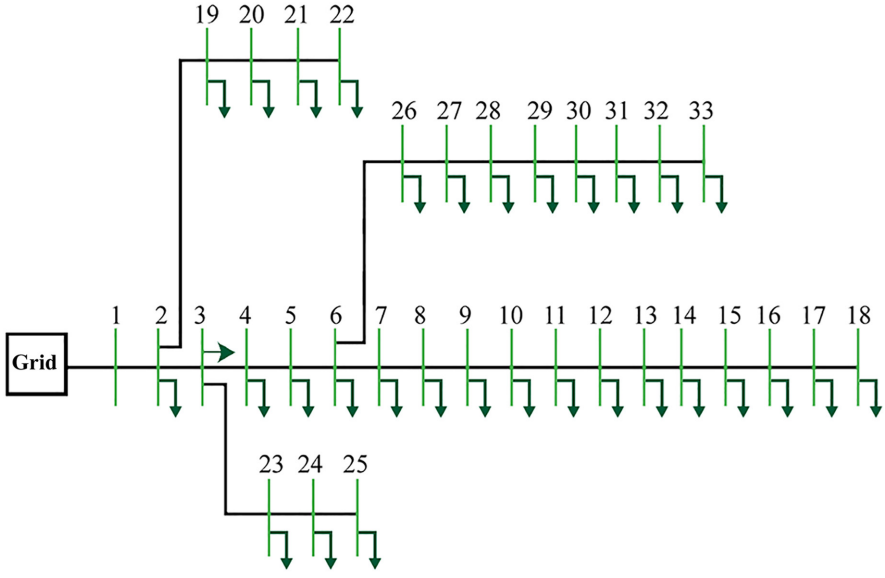

Fig. 4. IEEE 33 bus test system.

TABLE I.
COMPARISON OF BUS VOLTAGES OF DLF TECHNIQUE WITH OTHER POWER FLOW TECHNIQUES FOR IEEE-33 BUS TEST SYSTEM

Bus No.	DLF Method (p.u.)	Analytical Method (p.u.)[14]	Dynamic Data Matrix Method (p.u.) [29]	Direct Backward/ Forward Sweep Technique (p.u.) [30]
1	1.0	1.0000	1.0000	1.0000
2	0.9970	0.9970	0.9970	0.9970
3	0.9829	0.9829	0.9829	0.9829
4	0.9754	0.9754	0.9755	0.9754
5	0.9680	0.9680	0.9681	0.9679
6	0.9496	0.9496	0.9497	0.9494
7	0.9461	0.9461	0.9462	0.9459
8	0.9413	0.9412	0.9413	0.9322
9	0.9350	0.9350	0.9351	0.9259
10	0.9292	0.9292	0.9292	0.9200
11	0.9283	0.9283	0.9284	0.9192
12	0.9268	0.9268	0.9269	0.9177
13	0.9207	0.9207	0.9208	0.9115
14	0.9185	0.9185	0.9185	0.9092
15	0.9170	0.9171	0.9171	0.9078
16	0.9157	0.9157	0.9157	0.9064
17	0.9136	0.9137	0.9137	0.9043
18	0.9130	0.9131	0.9131	0.9037
19	0.9965	0.9965	0.9965	0.9964
20	0.9929	0.9929	0.9929	0.9929
21	0.9922	0.9922	0.9922	0.9922
22	0.9915	0.9916	0.9916	0.9915
23	0.9793	0.9793	0.9794	0.9792
24	0.9726	0.9727	0.9727	0.9726
25	0.9693	0.9693	0.9694	0.9692
26	0.9477	0.9477	0.9477	0.9475
27	0.9451	0.9451	0.9452	0.9449
28	0.9337	0.9338	0.9337	0.9335
29	0.9255	0.9256	0.9255	0.9253
30	0.9219	0.9220	0.9220	0.9217
31	0.9177	0.9178	0.9178	0.9175
32	0.9168	0.9169	0.9169	0.9166
33	0.9165	0.9166	0.9166	0.9163

DLF, distribution load flow.

TABLE II.
SUMMARY OF POWER LOSS RESULTS FOR DIFFERENT METHODS

Method	Total Active Power Loss (kW)
DLF method	202.677
The new analytical formulation [14]	202.771
Dynamic data matrix method [29]	202.7
The direct backward/forward sweep technique [30]	211

DLF, distribution load flow.

discharge power for all BESS, respectively. $\sum_{n=1}^{N_{PV}} P_t^{PV}$ defines the sum of generated power by all PV panels.

Battery energy storage systems have different efficiencies in charging and discharging modes. Therefore, discharge and charge powers are modeled as separate variables.

2) BESS Constraint

The charging/discharging processes of BESS simultaneously are prevented by using (22).

$$P_t^{BC}.P_t^{BD} = 0 \qquad \forall t \tag{22}$$

The state of charge (SoC) of a battery is its available capacity expressed as a percentage of its rated capacity.

$$SoC^{min} \le SoC_t^{BESS} \le SoC^{max} \qquad \forall t \tag{23}$$

where SoC^{min} and SoC^{max} are the lower and upper permissible SoC limits. In this study, SoC was determined as 20% lower limit and 80% upper limit.

3) Buying and Selling Constraint

An MG is prevented buying and selling electricity simultaneously at each time step by using (24).

$$P_t^{GB}.P_t^{GS} = 0 \qquad \forall t \tag{24}$$

4) Voltage Constraints

The bus voltages at each bus is bound by a specified lower and upper limit by (25).

$$V_i^{min} \le V_{i,t} \le V_i^{max} \qquad \forall t,i \tag{25}$$

V_i^{min} and V_i^{max} mean lower/upper permissible voltage limits.

The lower and upper voltage limits which are set at 0.9 p.u. and 1.1 p.u., respectively as follows: (26).

$$0.90(p.u) \le V_{i,t} \le 1.1(p.u) \qquad \forall t,i \tag{26}$$

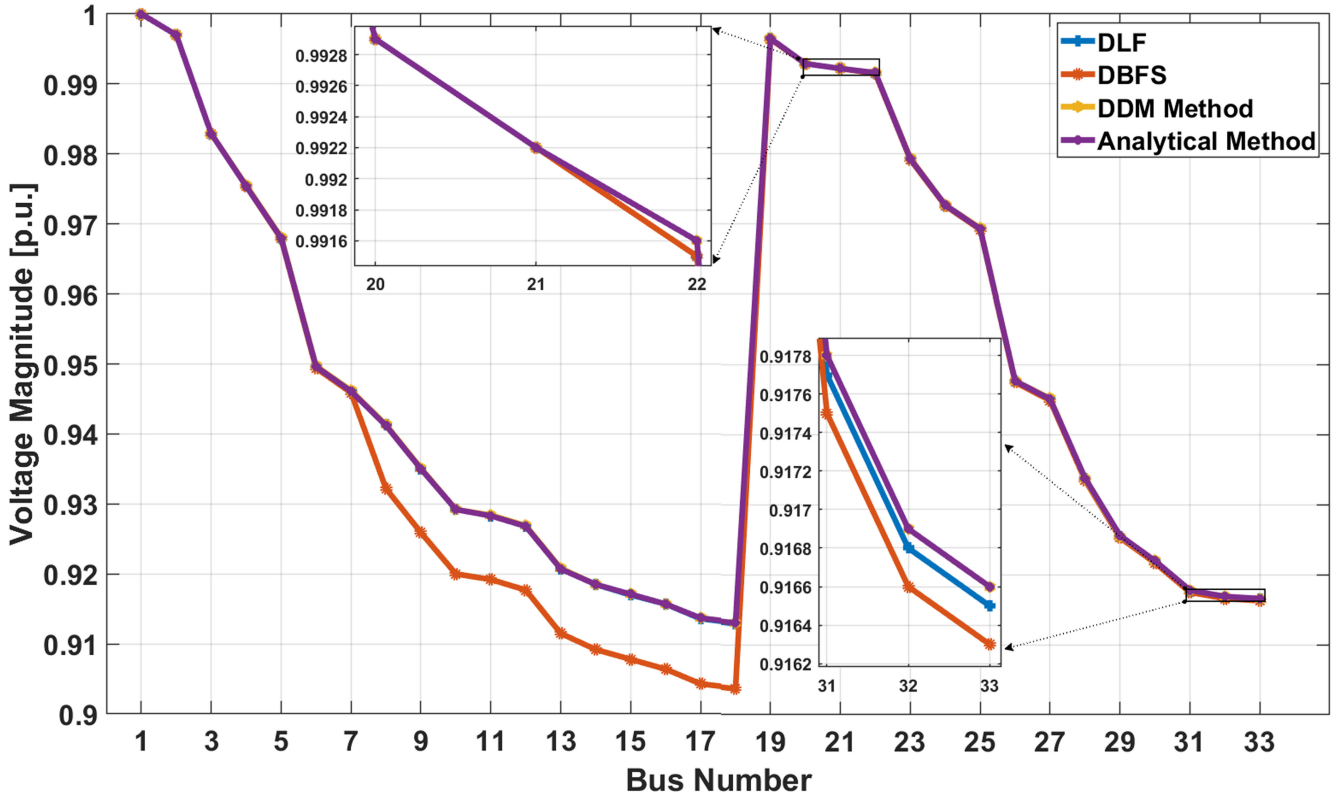

Fig. 5. Comparison of voltages at each bus for different power flow methods.

The final optimization problem takes the form as follows:

$$min\ F = \sum_{t=1}^{T}\left(\sum_{n=1}^{N_{BESS}}\left(P_t^{GB}.\lambda_t^{pp} - P_t^{GS}.\lambda_t^{SP} + P_t^{BC}.\beta_{CC} + P_t^{BD}.\beta_{DC}\right)\right).t \qquad \forall t,n \tag{27}$$

subject to (2)–(4) and (21)–(26).

The aim of this paper is to reduce the cost of energy bought from the grid and the operating costs of the BESSs and also to increase the energy sales to the grid.

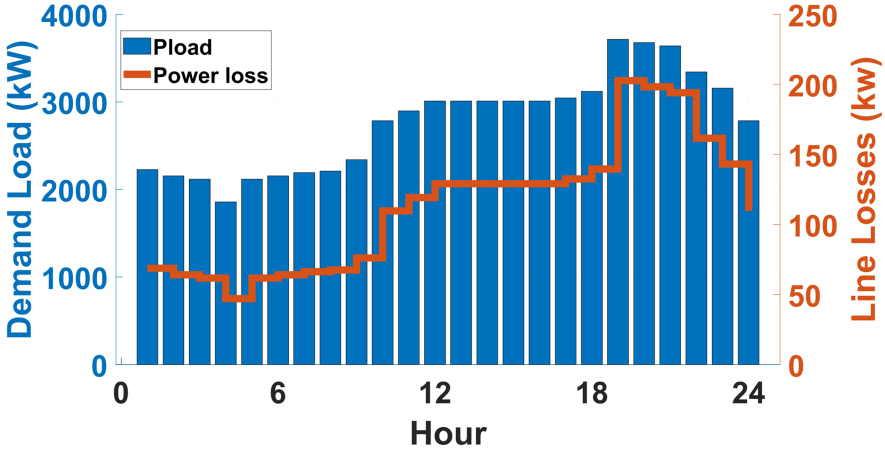

Fig. 6. Twenty-four-hour load profile and base case line losses.

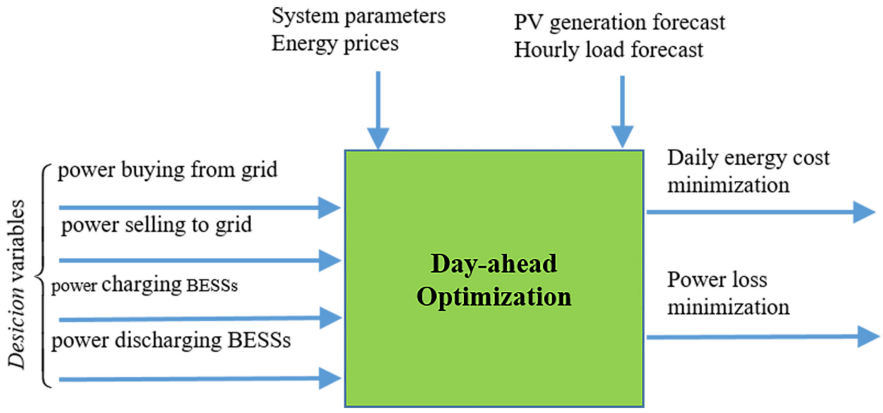

Fig. 7. Input–output scheme.

The last term (P_{Loss}) of the power balance equation given in (21) is obtained from PFC. Power flow calculation includes the set of nonlinear equations. Thus, the proposed day-ahead EMS scheduling transforms to a nonlinear optimization problem.

V. SIMULATION STUDIES AND RESULTS

A. System Configuration

The study aims at the lowest cost of energy by integrating PV and BESS in the test system. Moreover, revenues can be increased through more PV generations. Battery energy storage systems contribute to revenues or lower expense for buying energy from grid when the market prices are volatile. The modified test system in [32] is depicted in Fig. 8.

Photovoltaics and BESS parameters are shown in Table III and IV.

The proposed approach requires the forecast data of the loads, PV generations, and the spot price data of the grid. This study assumes that the PV generation forecasted by historical data is available for EMS. The placement problem of PV and BESS is beyond the scope of this paper, because we focus on the optimal operating of MG.

Fig. 9 illustrates the electrical energy price of buying and selling in day-ahead spot market.

The hourly variation of the power to be generated by the PV panels used in the day-ahead EMS and the total active power demand are demonstrated in Fig. 10.

B. Simulation Results

To assess practically the effects of integrating PV and BESS into the IEEE 33 bus test system, PV and BESS should be integrated separately.

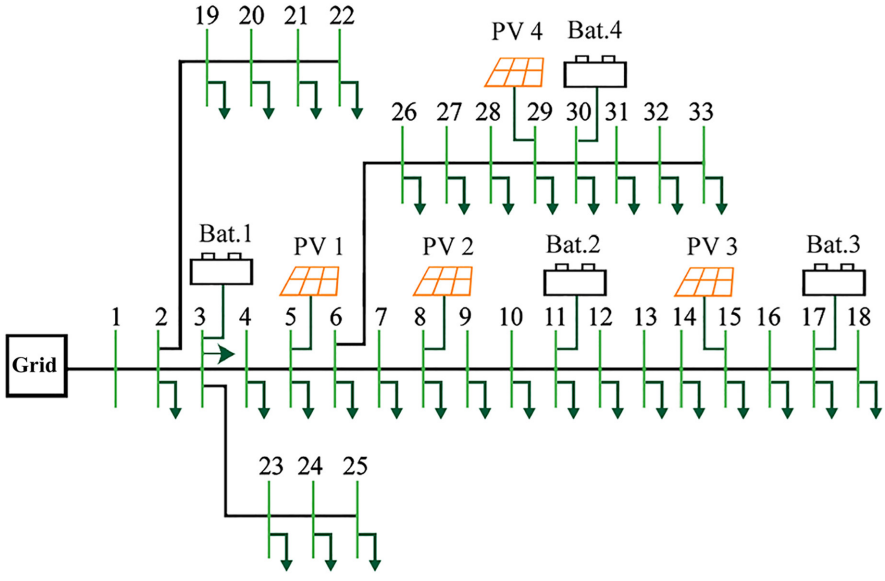

Fig. 8. IEEE 33 bus test system (modified from [33]).

TABLE III.
BESS PARAMETERS

Equipment	Location	Maximum Power (MW) [34] $\left(P^{BC,max}, P^{BD,max}\right)$	Maximum Capacity (MWh) [34] (SoC)	Charge Efficiency $\left(\eta_{BC}\right)$ [15]	Discharge Efficiency $\left(\eta_{BD}\right)$ [15]	Degradation Cost ($/kWh) $\left(\beta_{CC}, \beta_{DC}\right)$ [15]
BESS-1	Bus 3	2	2	0.95	0.90	0.042
BESS-2	Bus 11	1	1	0.95	0.90	0.042
BESS-3	Bus 17	1	1	0.95	0.90	0.042
BESS-4	Bus 30	2	2	0.95	0.90	0.042

BESS, battery energy storage system.

Therefore, only PVs are integrated first, and then only BESSs are integrated and finally both PVs and BESSs are integrated simultaneously the last.

Case 1: Only PVs are integrated,

Case 2: Only BESSs are integrated,

Case 3: Both PVs and BESSs are integrated.

Nonlinear programming solver, MATLAB's fmincon solver, was used for finding the minimum of the nonlinear optimization problem in the case studies simulations.

1) Case 1
The demanded power by the load was supplied from both PV and grid instead of only from grid. The cost of energy was calculated as $3761. Thus, the cost was reduced to approximately 56% compared to the base case. Moreover, the daily energy loss was calculated as 2442 kWh. Hence, approximately 10% daily energy loss reduction was achieved when compared with the base case.

2) Case 2
Only the BESSs were integrated in the system, and the cost of energy for 1 day was calculated as $8507. This shows a reduction of 2% in the cost of energy compared to the base case. Furthermore, the energy loss was calculated as 2628 kWh, with a decrease of 4% compared to the base case.

TABLE IV.
PV GENERATION SYSTEM PARAMETERS

Equipments	Location	Rated Power (MW) (P_r^{PV})	Panel Area (m²) $\left(A_{pv}\right)$	Panel Efficiency $\left(\eta_{pv}\right)$
PV-1	Bus 5	1	5000	0.20
PV-2	Bus 8	0.8	4000	0.20
PV-3	Bus 15	1.2	6000	0.20
PV-4	Bus 29	1.4	7000	0.20

PV, photovoltaic.

3) Case 3
In the last case, by integrating both the PVs and the BESSs into the MG, the cost of energy was obtained as $3646, which resulted in an energy cost advantage of approximately 58%.

The results described above are that the objective function is to minimize the cost of energy. Different case studies, such as by integrating only PVs, only BESSs, and both PVs and BESSs into the test system, are carried out to investigate the effects of the aim of objective function in each case on the cost of energy and the energy loss in order to reveal the differences of the costs and the losses. To summarize

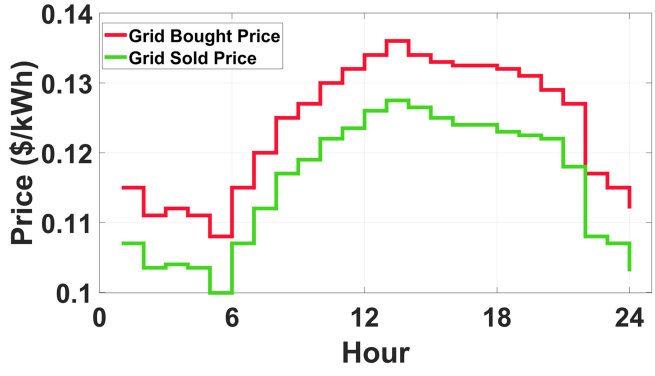

Fig. 9. Day-ahead purchase and sales electricity prices [12].

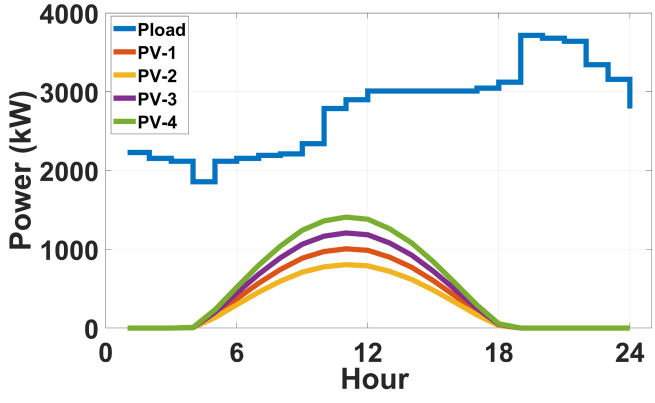

Fig. 10. Load [32] and PV power [34] profile.

TABLE V.
COMPARISON OF CASE STUDIES RESULTS

Outputs	Base Case		Case 1		Case 2		Case 3	
	OF-1	OF-2	OF-1	OF-2	OF-1	OF-2	OF-1	OF-2
Cost ($)	8660	8660	3761	3761	8507	8566	3646	3938
Losses (kWh)	2733	2733	2442	2442	2628	2606	2312	1955
Time (s)	25	34	35	23	1058	931	864	728

OF-1, the objective function is to determine cost; OF-2, the objective function is to determine energy loss.

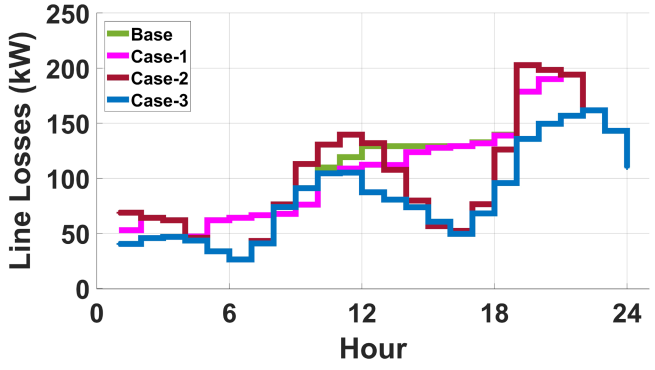

Fig. 11. Hourly variation of total line losses.

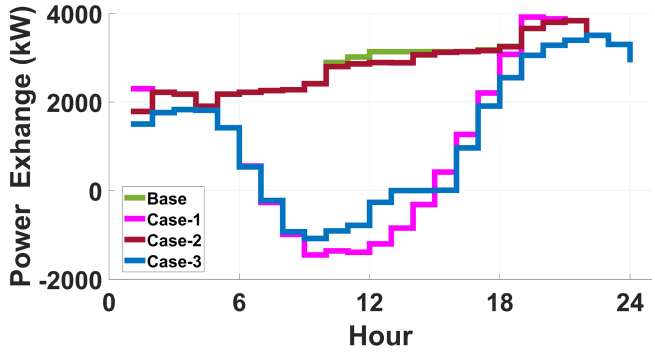

Fig. 12. The comparison of power exchange to grid.

briefly, it is simulated with two different objective functions: the objective function is to determine cost (OF-1) and the objective function is to determine energy loss (OF-2). The simulation results of different objective functions are given separately in Table V.

In case 2, the energy loss was calculated as 2606 kWh in the case whose objective function was to minimize energy loss, while energy loss was 2628 kWh in the case whose objective function was to minimize the energy cost. Here, an important feature is that energy loss can change according to the objective function. Moreover, the cost of energy was decreased from $8566 to $8507 compared to the objective function which was to minimize the energy loss. This implies to supply energy from the BESS instead of of purchase energy the grid, which increases more line loss. The demand loads are supplied by the BESS in order to minimize the energy cost.

Similarly, in case 3, although the energy loss increased, the total energy cost was calculated as lower when the objective function was

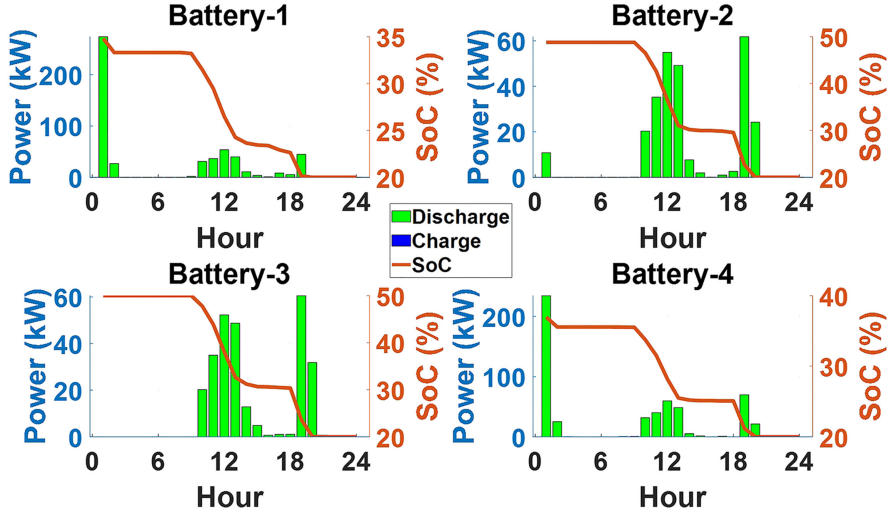

Fig. 13. Battery energy storage system power and SoC at case 2.

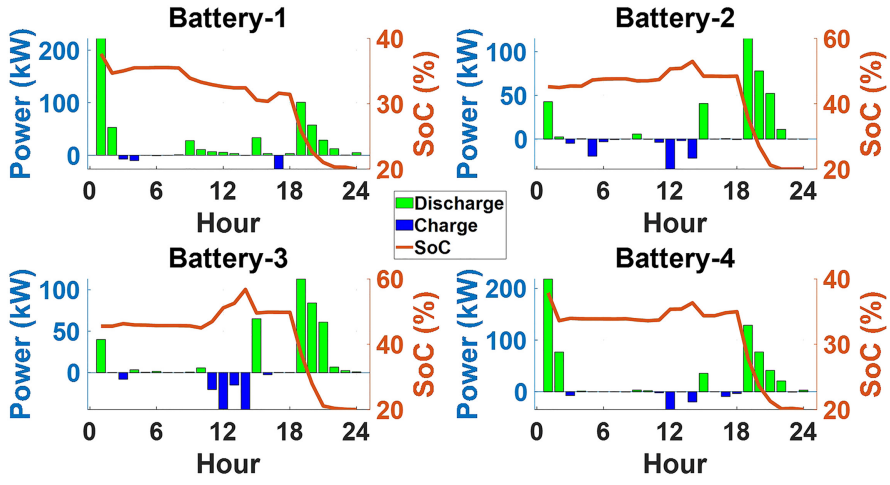

Fig. 14. Battery energy storage system power and SoC at case 3.

to minimize the energy cost. All analyses in the following parts of the study have been considered as objective function to minimize the cost of energy. Figs 11 and 12 give the line losses and energy exchange with grid according to the cases, respectively.

Fig. 13 illustrates the charge/discharge power and also SoC of the BESS in case 2.

The demand loads were supplied from the BESSs in order to get the highest profits when purchase prices are highest. Similarly, when the load was at the peak level, the loads were supplied by BESS; thus, the cost of energy was reduced. Battery energy storage systems discharged power until SoC reached 20%, which was the lower energy limit of BESS.

The powers and SoC of BESSs are seen in case 3 in Fig. 14. The BESSs kept a large amount of its energy until the evening when the load and market price were high. The BESSs discharged power until they emptied own energies.

The bus voltages given in Fig. 15 are obtained by solving the PFC according to the case studies.

Because the buses 6, 13, and 31 were near the PV system, the voltage fluctuation was caused by the PV power. Therefore, it was seen that bus voltage fluctuation was very high compared to the other buses.

Rise in bus voltage profiles in case 1 and case 3 were observed at noon by considering the generation of PV after integrating the PV to test system. The bus voltage magnitudes in case 3 were less than that in case 2 due to decreasing bus voltages because of the BESS in charging mode acting like a load. Voltage magnitudes at the specified buses were improved with BESS integration. Improvement in bus voltages at nearly all buses can be seen in case 2 compared to the base case especially around noon. The BESS injected the power into MG instead of buying from the grid, improving the voltage level due to the high energy price of purchase from the grid. Minimum bus voltage deviation was seen at bus 22 due to the fact that there is not any integration of PV or BESS between bus 22 and the grid bus.

C. Sensitivity Analysis

A comprehensive sensitivity analysis is performed to assess the robustness and sensitivity of the system. Solar irradiation is an important parameter that affects the cost of energy. The solar irradiation is historical data for the period from January 1, 2006, to December 31, 2006, in İzmir/ Turkey (38.471N, 27.169E) for

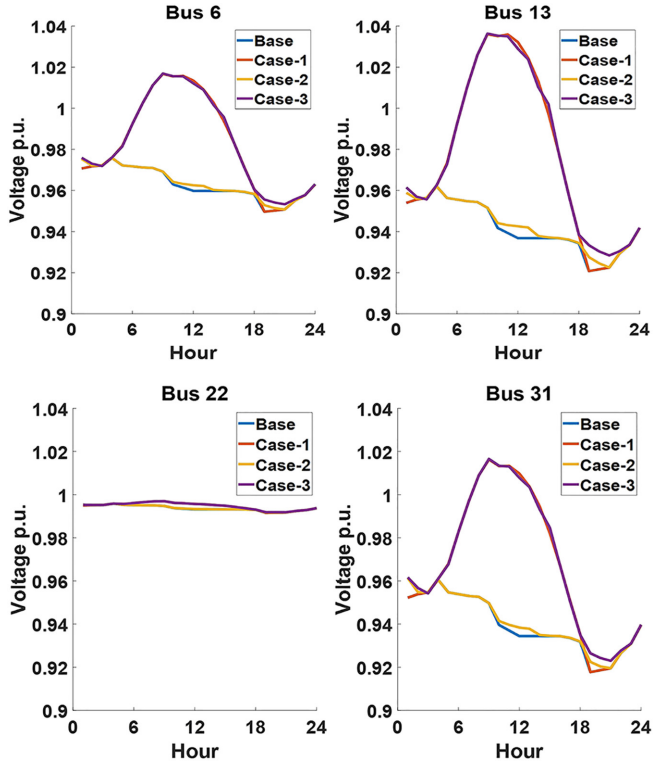

Fig. 15. Bus 6, 13, 22 and 31 voltage profile according to case studies.

sensitivity analysis [33]. Fig. 16 shows the solar energy profile illustrating the amount of solar radiation in different days of a year for the selected location. It is evident that on the summer days, there is more solar irradiance than on the winter days. This difference affects the cost of energy.

To evaluate this parameter, the modified system was modeled and simulated based on the values of the daily weather data, which implies the best and worst weather conditions like the cloudy winter and clear summer days.

The cost of energy and the power loss are given in Table VI, which are obtained from the simulation results for the modified IEEE 33 bus test system.

The cost of energy was calculated as the lowest level since PV generation was at maximum levels on a clear summer day, which was the day with the highest irradiance. On the other hand, the lowest irradiance day, which was a partially cloudy winter, was calculated as the highest energy cost. With regard to energy loss, the highest energy loss was calculated on a partially cloudy winter day, while the lowest energy loss was calculated on a partially cloudy summer day.

TABLE VI.
COMPARISON OF ENERGY COST AND LOST ENERGY FOR DIFFERENT DAYS

Types of Day	Cost ($)	Energy Loss (kWh)
Clear summer	3646	2312
Clear winter	6970	2163
Partially cloudy summer	4727	2255
Partially cloudy winter	7449	2246

Other important factors affecting the cost of energy and the power loss are electricity price, PV capacity powers, and degradation costs.

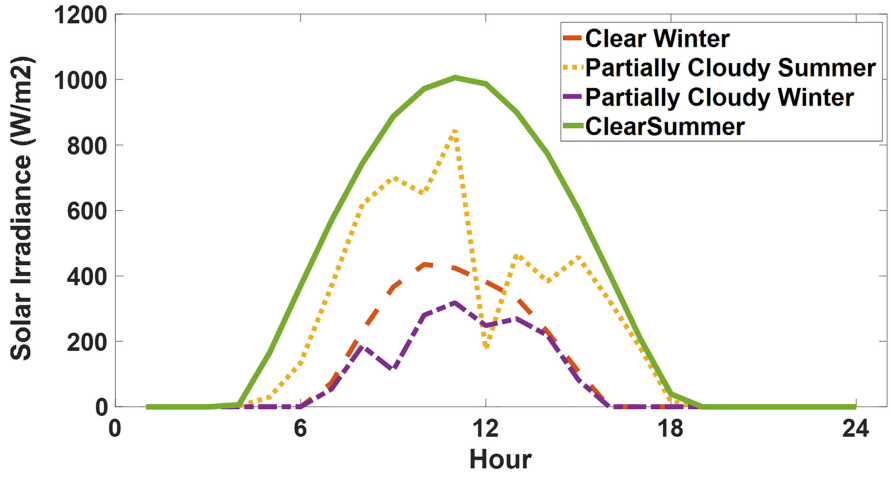

Fig. 16. Solar irradiance for four selected days.

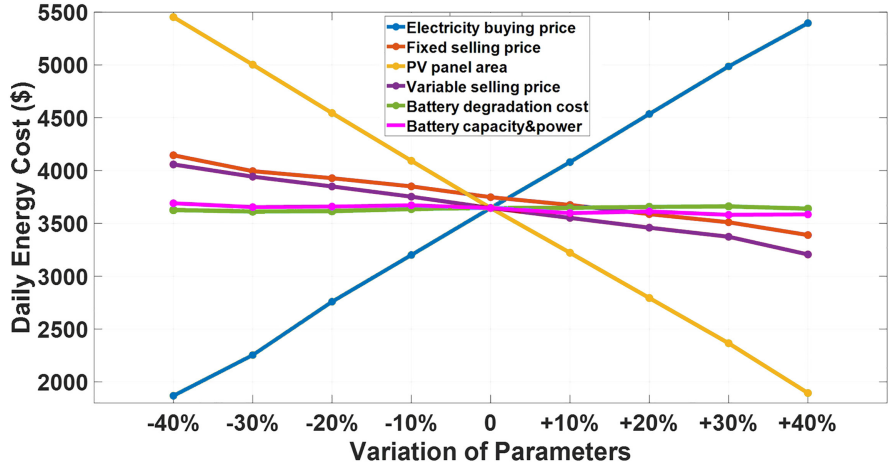

Fig. 17. Daily energy cost versus variation of parameters.

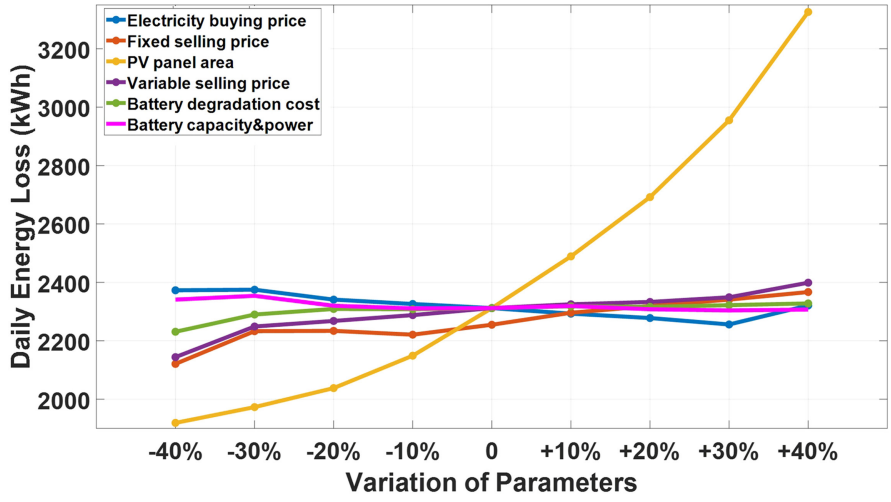

Fig. 18. Daily energy loss versus variation of parameters.

The day-ahead EMS uses electricity purchase price, electricity variable/fixed selling price, PV panel area, BESS degradation cost, BESS capacity, and power for six different sensitivity cases.

Figs 17 and 18 show the sensitivity analysis results of the daily cost of energy and the daily energy loss. The fixed selling price means that the feed-in rate is assumed as 0.11$/kWh for the entire day.

This sensitivity analysis was performed with the system configuration specified in case 3 and on a clear summer day. The results reveal that two most important parameters affecting the daily energy cost are electricity purchase price and the energy generated by PV panels.

As anticipated, the daily energy cost becomes lower as the fixed and variable selling prices increase. It is seen that the capacity, the power, and the degradation cost of the BESS are the parameters that affect the daily energy cost the least.

In terms of daily energy loss, an increase in the area of PV panels, which means an increase in the amount of energy generated by PV panel, increases the energy loss. When the electricity sales prices increased, the loss of energy increased slightly due to a slight increase in the sales to the grid. Because of the increase in the price of the energy bought from the grid, the amount of energy bought from the grid reduced. So, the energy loss decreased.

VI. CONCLUSION

The increase in the diversity of DG resources and in the number of equipment used, such as BESSs and PV systems, complicates the problem that needs to be solved in the day-ahead EMS. Energy management system is the practical way of decreasing the cost of energy and ensuring the technical limits of MG. With the nonlinear equation, sets were formulated in this study and by means of these formulations, EMS scheduling problem was solved for a base IEEE 33 bus test system. Then, case studies were carried out by creating a system with the addition of only PVs to the system. Later, only BESSs and finally both PVs and BESS were integrated into the MG.

The analyses in which the energy costs of the objective functions were minimized and in which the energy losses were minimized in four different case studies were made. It showed that the hybrid system configuration in which PV and BESS integrated to MG is the the lowest cost system configuration in terms of daily cost of energy and line loss. Moreover, the addition of BESS provided advantage on the cost and energy loss as well as improvements in the voltage profile. Then, the energy cost and energy loss were calculated on cloudy or non-cloudy days in summer and winter months using the realistic data of different irradiance.

As expected, the lowest energy cost was calculated during the clear summer day, whereas the highest energy cost was calculated on a cloudy winter day. In the sensitivity analysis, it was seen that the most impact on the daily energy cost was the cost of purchasing electricity and the PV panel area. Similarly, it was evaluated that the parameter affecting the energy loss the most was the PV panel area.

Peer-review: Externally peer-reviewed.

Declaration of Interests: The authors declare that they have no competing interest.

Funding: This study received no funding.

REFERENCES

1. REN21, *Renewables 2022 Global Status*. Paris: REN21 Secretariat, 2022. ISBN 978-3-948393-04-5.
2. G. Pepermans, J. Driesen, D. Haeseldonckx, R. Belmans, and W. D'haeseleer, "Distributed generation: Definition, benefits and issues," *Energy Policy*, vol. 33, no. 6, pp. 787–798, 2005. [CrossRef]
3. M. Fathi, and H. Bevrani, "Statistical cooperative power dispatching in interconnected microgrids," *IEEE Trans. Sustain. Energy*, vol. 4, no. 3, pp. 586–593, 2013. [CrossRef]
4. K. P. Kumar, and B. Saravanan, "Day ahead scheduling of generation and storage in a microgrid considering demand Side management," *J. Energy Storage*, vol. 21, pp. 78–86, 2019. [CrossRef]

5. J. A. Martinez, and J. Mahseredjian, "Load flow calculations in distribution systems with distributed resources. A review," in 2011 IEEE Power and Energy Society General Meeting, pp. 1–8, 2011. [CrossRef]
6. B. V. S. Vardhan, M. Khedkar, and I. Srivastava, "Effective energy management and cost effective day ahead scheduling for distribution system with dynamic market participants," *Sustain. Energy Grids Netw.*, vol. 31, p. 100706, 2022. [CrossRef]
7. M. Rahimi, F. J. Ardakani, O. Olatujoye, and A. J. Ardakani, "Two-stage interval scheduling of virtual power plant in day-ahead and real-time markets considering compressed air energy storage wind turbine," *J. Energy Storage*, vol. 45, p. 103599, 2022. [CrossRef]
8. G. Huang, H. Wu, Z. Feng, Y. Ding, and J. Wang, "Day-ahead reactive-voltage optimization for active distribution network with energy storage," in 2021 3rd International Conference on Electrical Engineering and Control. Technologies (CEECT), 2021, pp. 170–174. [CrossRef]
9. X. Sun, J. Qiu, Y. Yi, and Y. Tao, "Cost-effective coordinated voltage control in active distribution networks with photovoltaics and mobile energy storage systems," *IEEE Trans. Sustain. Energy*, vol. 13, no. 1, pp. 501–513, 2022. [CrossRef]
10. J. H. Teng, "A direct approach for distribution system load flow solutions," *IEEE Trans. Power Deliv.*, vol. 18, no. 3, pp. 882–887, 2003. [CrossRef]
11. V. Vita, "Development of a decision-making algorithm for the optimum size and placement of distributed generation units in distribution networks," *Energies*, vol. 10, no. 9, p. 1433, 2017. [CrossRef]
12. F. H. Aghdam, N. T. Kalantari, and B. Mohammadi-Ivatloo, "A chance-constrained energy management in multi-microgrid systems considering degradation cost of energy storage elements," *J. Energy Storage*, vol. 29, p. 101416, 2020. [CrossRef]
13. A. Waqar *et al.*, "Analysis of optimal deployment of several DGs in distribution networks using plant propagation algorithm," *IEEE Access*, vol. 8, pp. 175546–175562, 2020. [CrossRef]
14. R. Srinivasa Rao, S. V. L. Narasimham, M. Ramalinga Raju, and A. Srinivasa Rao, "Optimal network reconfiguration of large-scale distribution system using harmony search algorithm," *IEEE Trans. Power Syst.*, vol. 26, no. 3, pp. 1080–1088, 2011.
15. H. A. Taha, M. H. Alham, and H. K. M. Youssef, "Multi-objective optimization for optimal allocation and coordination of wind and solar DGs, BESSs and capacitors in presence of demand response," *IEEE Access*, vol. 10, pp. 16225–16241, 2022. [CrossRef]
16. U. Sur, "Impact study of distributed generations in voltage sag mitigation using an improved three-phase unbalanced load flow for active distribution network," *Turk. J. Electr. Power Energy Syst.*, vol. 2, no. 2, pp. 124–133, 2022. [CrossRef]
17. S. Gupta, V. K. Yadav, and M. Singh, "Optimal allocation of capacitors in radial distribution networks using Shannon's entropy," *IEEE Trans. Power Deliv.*, vol. 37, no. 3, pp. 2245–2255, 2022. [CrossRef]
18. S. Koohi-Fayegh, and M. A. Rosen, "A review of energy storage types, applications and recent developments," *J. Energy Storage*, vol. 27, p. 101047, 2020. [CrossRef]
19. S. Bacha, D. Picault, B. Burger, I. Etxeberria-Otadui, and J. Martins, "Photovoltaics in microgrids: An overview of grid integration and energy management aspects," *IEEE Ind. Electron. Mag.*, vol. 9, no. 1, pp. 33–46, 2015. [CrossRef]
20. S. Polat, E. Bıyık, and H. Şekerci Öztura, "Batarya ve PV Sistemi İçeren Bir Mikro Şebekenin Gün Öncesi Enerji Yönetim Sistemi ile Optimum İşletilmesi," in CIGRE Türkiye - III. Power Systems Conference, GSK 2022. Ankara, 2022.
21. D. T. Ton, and M. A. Smith, "The U.S. Department of Energy's microgrid initiative," *Electr. J.*, vol. 25, no. 8, pp. 84–94, 2012. [CrossRef]
22. "Microgrids State working group | NASEO." [Online]. Available: https://www.naseo.org/issues/electricity/microgrids. [Accessed: December 9, 2022].
23. A. Dolara, S. Leva, and G. Manzolini, "Comparison of different physical models for PV power output prediction," *Sol. Energy*, vol. 119, pp. 83–99, 2015. [CrossRef]
24. T. Ma, H. Yang, and L. Lu, "Solar photovoltaic system modeling and performance prediction," *Renew. Sustain. Energy Rev.*, vol. 36, pp. 304–315, 2014. [CrossRef]
25. M. R. B. Khan, R. Jidin, and J. Pasupuleti, "Multi-agent based distributed control architecture for microgrid energy management and optimization," *Energy Convers. Manag.*, vol. 112, pp. 288–307, 2016. [CrossRef]
26. S. Cao, H. Zhang, K. Cao, M. Chen, Y. Wu, and S. Zhou, "Day-ahead economic optimal dispatch of microgrid cluster considering shared energy storage system and P2P transaction," *Front. Energy Res.*, vol. 9, 2021. [CrossRef]
27. K. Prakash, and M. Sydulu, "Topological and primitive impedance based load flow method for radial and weakly meshed distribution systems," *Iran. J. Electr. Comput. Eng.*, vol. 10, no. 1, pp. 10–18, 2011.
28. T. Thakur, and J. Dhiman, "A new approach to load flow solutions for radial distribution system," in 2006 IEEE PES Transmission and Distribution Conference and Exposition: Latin America, TDC'06, pp. 1–6, 2006. [CrossRef]
29. M. V. Kirthiga, S. A. Daniel, and S. Gurunathan, "A methodology for transforming an existing distribution network into a sustainable autonomous micro-grid," *IEEE Trans. Sustain. Energy*, vol. 4, no. 1, pp. 31–41, 2013. [CrossRef]
30. W. A. Vasquez, and F. L. Quilumba, "Load flow method for radial distribution systems with distributed generation using a dynamic data matrix," 2016 IEEE Ecuador Technical Chapters Meeting, ETCM 2016, pp. 16–20, 2016. [CrossRef]
31. G. Diaz, J. Gomez-Aleixandre, and J. Coto, "Direct backward/forward sweep algorithm for solving load power flows in AC droop-regulated microgrids," *IEEE Trans. Smart Grid*, vol. 7, no. 5, pp. 2208–2217, 2016. [CrossRef]
32. T. Tewari, A. Mohapatra, and S. Anand, "Coordinated control of OLTC and energy storage for voltage regulation in distribution network with high PV penetration," *IEEE Trans. Sustain. Energy*, vol. 12, no. 1, pp. 262–272, 2021. [CrossRef]
33. X. Li, L. Wang, N. Yan, and R. Ma, "Cooperative dispatch of distributed energy storage in distribution network with PV generation systems," *IEEE Trans. Appl. Supercond.*, vol. 31, no. 8, pp. 1–4, 2021. [CrossRef]
34. "JRC Photovoltaic Geographical Information System (PVGIS) - European Commission." [Online]. Available: https://re.jrc.ec.europa.eu/pvg_tools/en/#api_5.2. [Accessed: December 2, 2022].